CONFIDENTIAL

Copy 377
RM L55L21a

NACA

CASE FILE COPY

RESEARCH MEMORANDUM

LOW-SPEED STATIC STABILITY CHARACTERISTICS OF A CAMBERED-DELTA-WING MODEL

By John M. Riebe and William C. Moseley, Jr.

Langley Aeronautical Laboratory
Langley Field, Va.

CLASSIFICATION CHANGED TO UNCLASSIFIED
AUTHORITY: NACA RESEARCH ABSTRACT NO. 123
EFFECTIVE DATE: DECEMBER 13, 1957 WHL

CLASSIFIED DOCUMENT

This material contains information affecting the National Defense of the United States within the meaning of the espionage laws, Title 18, U.S.C., Secs. 793 and 794, the transmission or revelation of which in any manner to an unauthorized person is prohibited by law.

NATIONAL ADVISORY COMMITTEE
FOR AERONAUTICS

WASHINGTON

March 8, 1956

CONFIDENTIAL

NATIONAL ADVISORY COMMITTEE FOR AERONAUTICS

RESEARCH MEMORANDUM

LOW-SPEED STATIC STABILITY CHARACTERISTICS OF A CAMBERED-DELTA-WING MODEL

By John M. Riebe and William C. Moseley, Jr.

SUMMARY

An investigation was made in the Langley 300 MPH 7- by 10-foot tunnel to determine the static stability characteristics of a cambered-delta-wing model. The cambered delta wing was derived from a segment of a cone selected so that the projected plan form with a wing dihedral angle of 0° was the same as a 60° delta wing. The projected plan form had an aspect ratio of 2.31.

The tail-off longitudinal stability for the model with wing dihedral angles of 0°, 20°, 33°, and 50° was very similar to that of the plain delta wing. Increasing the wing dihedral angle from 0° to 50° with tail off resulted in increased static directional stability with increase in lift coefficient. However, increasing the wing dihedral with tail off resulted in a rapid decrease in the effective dihedral at high lift coefficients. Proper selection of V-tails which were investigated with the 20° and 50° wing dihedral angles resulted in model configurations which had longitudinal and directional stability throughout the lift-coefficient range. However, slight losses in effective dihedral occurred at the higher lift coefficients.

INTRODUCTION

Experiment and theory have shown that some structural and aerodynamic advantages can be obtained on airplanes through the use of the delta wing. However, a serious problem on airplanes using this plan form has been a loss of directional stability and effective dihedral at high angles of attack. (See ref. 1.) It has been shown that a possible method of reducing the lateral stability problem is through the use of twist and camber (ref. 2) or through the use of geometric dihedral (ref. 3). In addition, the use of twist and camber in delta wings has provided increases in the lift-drag ratio through elimination of leading-edge separation both at subsonic speeds (ref. 4) and at supersonic speeds (ref. 5).

The present paper gives the results of an investigation made in an attempt to eliminate the lateral stability problems of delta wings at high angles of attack through the use of a delta wing derived from a segment of a cone. The conical configuration was suggested as a possible method of offering the advantages of twisted and cambered delta wings with a simplified method of construction. Use of the conical configuration might find particular application in guided missile wings with construction consisting of conical rolling of sheet metal. In addition to advantages of simplified construction the configuration might be a method of providing structural stiffness to wings of thin airfoil sections.

In the present low-speed static stability investigation, the conical delta wing was investigated on a fuselage at dihedral angles of 0°, 20°, 33°, and 50°. A delta vertical tail and a V-tail at various dihedral angles were also investigated to determine the effect on the longitudinal and lateral stability of the configuration with two of the more promising wing-dihedral angles.

SYMBOLS

The data are presented in the form of standard NACA coefficients of forces and moments and are referred to the stability axes with the origin at the quarter-chord point of the mean aerodynamic chord. The coefficients are based on the projected plan form of the wing at 0° and 33° dihedral angle which has the same dimension of a delta wing with 60° apex angle. The positive directions of the forces, moments, and angular displacements are shown in figure 1, the coefficients and symbols used herein are defined as follows:

C_L	lift coefficient, Lift/qS
C_D	drag coefficient, D/qS
C_Y	lateral-force coefficient, Y/qS
C_m	pitching-moment coefficient, $M/qS\bar{c}$
C_n	yawing-moment coefficient, N/qSb
C_l	rolling-moment coefficient, L/qSb
Z	force along Z-axis (lift equals -Z), lb
D	drag (-X when $\beta = 0^\circ$), lb
X	force along X-axis, lb

Y	force along Y-axis, lb
M	pitching moment, ft-lb
N	yawing moment, ft-lb
L	rolling moment, ft-lb
q	free-stream dynamic pressure, $\frac{\rho V^2}{2}$, lb/sq ft
S	wing area, 6.93, sq ft
$\bar{c}$	wing mean aerodynamic chord, $\frac{2}{S}\int_0^{b/2} c^2 dy$, 2.31 ft
b	wing span, 4.00 ft
ρ	mass density of air, slugs/cu ft
V	free-stream velocity, ft/sec
c	local wing chord, ft
y	lateral distance from plane of symmetry measured parallel to Y-axis, ft
α	angle of attack of reference axis (fig. 1), deg
β	angle of sideslip, deg
Γ_W	wing dihedral (measured in plane tangent to wing surface at wing root; see fig. 2)
Γ_T	tail dihedral (fig. 4)

$$C_{L_\alpha} = \left(\frac{\partial C_L}{\partial \alpha}\right)_{\beta=0}$$

$$C_{l_\beta} = \left(\frac{\partial C_l}{\partial \beta}\right)_{\alpha}$$

$$C_{n_\beta} = \left(\frac{\partial C_n}{\partial \beta}\right)_{\alpha}$$

$$C_{Y_\beta} = \left(\frac{\partial C_Y}{\partial \beta}\right)_{\alpha}$$

The subscripts α and β indicate the factor held constant.

The slope C_{L_α} was measured at zero angle of attack.

APPARATUS AND MODEL

The model was tested in the Langley 300 MPH 7- by 10-foot tunnel on a single strut. The general arrangement of the wing and the dihedral angles tested are shown in figure 2. The geometric dimensions of the wing were selected so that the projected plan form would be triangular with a 60° apex angle at dihedral angles of 0° and 33°. The projected plan form had an aspect ratio of 2.31 and an area of 6.93 square feet. The wing area was selected so that a comparison could be made with the plain 60° triangular wing previously investigated in references 6 and 7. The wing semispans were made of 1/8-inch sheet steel formed into a cambered shape. The desired shape was obtained by using a segment of a right circular cone for each semispan (fig. 3). The leading edge of the wing was an element of the cone 39.87 inches in length. The amount of camber obtainable was defined by the height and the radius of the base of the cone. For the present tests a cone height of 31.06 inches and a radius of 25.00 inches were used. The wing was tested at dihedral angles of 0°, 20°, 33°, and 50° measured in the plane tangent to the wing at the intersection with the fuselage (fig. 2). As mentioned previously, all computations were based on a projected area of 6.93 square feet. The wing leading and trailing edges were rounded.

The fuselage used during the investigation had a circular section and was the same as used in a previous investigation (ref. 7).

Dimensions of the tail and tail-dihedral angles tested on the model are shown in figure 4. The tails were flat plates constructed of 1/8-inch sheet aluminum and had rounded leading and trailing edges.

TEST CONDITIONS

The tests were made in the Langley 300 MPH 7- by 10-foot tunnel at a dynamic pressure of 25 pounds per square foot, corresponding to an airspeed of about 100 miles per hour. Mach number and Reynolds number for this airspeed, based on the mean aerodynamic chord (2.31) of the plain wing, were 0.13 and 2.1×10^6, respectively. The tests were made through the -6° to 35° angle-of-attack range. Because of the preliminary nature of the investigation, the lateral stability parameters were determined from tests at $\pm 5^\circ$ sideslip through the angle-of-attack range. However, a few

tests were made through the 5° to -30° sideslip range at 10° angle of attack.

Corrections.- Jet-boundary corrections applied to the data were obtained from the methods of reference 8. Blocking corrections have been applied to the data according to the methods outlined in reference 9. Buoyancy corrections have been applied to the data to account for a longitudinal static pressure gradient in the tunnel. The angles of attack have been corrected to account for air-stream inclination.

PRESENTATION OF RESULTS

The results are presented as follows:

RESULTS AND DISCUSSION

Longitudinal characteristics - tail off.- Longitudinal aerodynamic characteristics in pitch (fig. 5) show approximately the same lift-curve slope for the model with the conical wing at 0° and 33° dihedral angle $\left(C_{L_\alpha} \approx 0.047\right)$ as the lift-curve slope for the plain wing of reference 6 $\left(C_{L_\alpha} \approx 0.046\right)$. This was as expected since the projected plan form of the conical wing at 0° and 33° dihedral angle was the same as the plain wing.

With 50° wing dihedral, the lift-curve slope $\left(C_{L_\alpha} \approx 0.037\right)$ was about 20 percent lower than the plain wing. About two-thirds of this decrease could be attributed to the smaller (about 13 percent less) projected plan form (the data are based on the plain delta wing area). Some increase in lift-curve slope $\left(C_{L_\alpha} \approx 0.054\right)$ was noted for the 20° wing-dihedral-angle configuration. The angle of attack for zero lift for the conical wing at the various dihedral angles investigated was more positive compared to the slight positive angle for the plain-delta-wing configuration. The conical-delta-wing configurations were generally longitudinally stable throughout the lift-coefficient range and about the same as those of the plain delta wing (fig. 5).

Longitudinal characteristics - tail on.- Although the primary purpose of adding a tail to the model of the present investigation was to provide directional stability, and the resulting tail configurations were directed toward this end, some discussion will be made of the effects on the longitudinal stability. The results of tests made with a wing dihedral angle of 20° and various tail configurations are presented in figure 6(a). These pitching-moment data show that with the exception of the 45° tail-dihedral-angle configuration which was almost neutrally stable throughout the lift-coefficient range, the various tail configurations tested resulted in a stable variation throughout the lift-coefficient range. As would be expected, the delta vertical tail (designated 90° V-tail, fig. 6 shows a variation of pitching moment with lift very similar to the tail-off data. The data of figure 6(b) indicate that a -45° V-tail configuration with the wing at 50° dihedral was also stable throughout the lift-coefficient range investigated.

Lateral characteristics - effect of large sideslip angles.- A few tests were made to determine whether the variation of the lateral coefficients C_l, C_n, C_Y with sideslip angle β, had sufficient linearity so that the testing could be restricted to ±5° sideslip angles through the lift-coefficient range. Results at 10° angle of attack (fig. 7(a)) showed a general linear variation of these coefficients over the 5° to -30° sideslip angle range for the configuration with tail off. Addition of the delta vertical tail generally resulted in a linear variation of the coefficients through most of the sideslip-angle range, figure 7(b). A loss of stability occurred, however, over part of the high-sideslip-angle range depending on the wing-dihedral angle. Such effects are probably caused by passage of the vertical tail through the wake vortices of the wing.

Lateral characteristics through the lift-coefficient range - tail off.- Large effects with dihedral of the conical wing occurred on the variation of the lateral stability parameters C_{l_β}, C_{n_β}, and C_{Y_β} with lift coefficient (fig. 8). At low dihedral angles, the directional stability C_{n_β} became more unstable with lift coefficient. At the high

dihedral angles, the directional stability increased with lift coefficient. The primary cause of the increase can be attributed to an increase of lateral area of the wing behind the center of moments with increased wing dihedral which resulted also in increased C_{Y_β}. Similar effects have been noted in reference 3 when a plain wing was investigated through a dihedral-angle range. However, the more favorable directional stability at high angles of attack for the high-dihedral-angle-wing configuration can also be partly attributed to an effect of vertical location of the wing on the fuselage, reference 10, which showed that at high angles of attack high-wing-fuselage configurations (tail off) were less unstable directionally than low-wing-fuselage configurations.

Throughout most of the lift-coefficient range, increasing the geometric dihedral of the wing increased the effective dihedral C_{l_β} as would be expected. However, at high lift coefficients, the configurations with large dihedral angles had a rapid decrease of C_{l_β} with lift coefficient. For the low-dihedral-angle-wing configurations, where the projected plan form was about the same as the plain wing, the C_{l_β} decrease was delayed to higher lift coefficients. For the 0° wing-dihedral-angle configuration, the effective dihedral continued to increase with lift coefficient throughout the lift-coefficient range. These changes of C_{l_β} in the high lift-coefficient range are generally related to the maximum lift coefficients of the wing which were lower with the high-dihedral-angle-wing configurations, figure 5.

Lateral characteristics through the lift-coefficient range with vertical tail on.- The addition of the delta vertical tail generally increased the directional stability throughout the lift-coefficient range except at high lift coefficients where large reversals occurred in C_{n_β} (fig. 8). The increase of directional stability with the addition of the delta tail at low lift coefficients (figs. 8 and 9) was largest for the low-dihedral-angle wings.

The delta vertical tail increased the effective dihedral for the high-dihedral-angle-wing configurations throughout the lift-coefficient range, except at high lift coefficients where large reductions occurred (fig. 8). For the low-dihedral-angle-wing configurations, the addition of the delta tail resulted in a decrease in effective dihedral in the moderate lift-coefficient range, produced an increase at high lift coefficients (fig. 8), and had practically no effect near zero lift coefficient (figs. 8 and 9). One of the smallest variations of effective dihedral, which was also positive throughout the lift-coefficient range, occurred for the 20° wing-dihedral-angle configuration.

Effect of tail configuration on most promising wing-dihedral configurations.- In addition to providing directional stability and effective dihedral it is desirable that variations of these parameters throughout the lift-coefficient range be kept to a minimum. The configuration with 20° wing-dihedral angle, tail off, had one of the smallest variations of lateral stability parameters C_{n_β} and C_{l_β} with lift coefficient (fig. 8(a)). However, the configuration had directional instability throughout the lift-coefficient range. Attempts at providing directional stability by means of a delta-vertical tail have been shown to be unsatisfactory because of the large loss in directional stability at high lift coefficients. Therefore the 20°-wing-dihedral-angle configuration was also investigated with various dihedral angle V-tail configurations consisting of two delta panels, each having the same plan form as the delta-vertical tail. Results of tests of the tail at various dihedral angles are presented in figure 10. The large loss of directional stability of the delta-vertical-tail configuration (identified as 90° V-tail configuration, fig. 10) was reduced or completely eliminated with the V-tails at the lower dihedral angles, but the configurations still were directionally unstable in the low-lift-coefficient range.

The configuration consisting of a horizontal tail (0° V-tail configuration) had a variation of effective dihedral with lift coefficient that varied more uniformly and did not have an abrupt decrease at high lift coefficients compared to the tail-off configuration. As might be expected, the horizontal tail had practically no effect in reducing the directional instability in the low-lift-coefficient range. However, at high-lift coefficients the 0° V-tail configuration had less directional instability than the tail-off configurations.

One of the smallest variations of C_{n_β} and C_{l_β} with lift coefficient occurred for the 20°-wing-dihedral-angle configuration with 30° tail dihedral, figure 10, although directional instability occurred in the low-lift-coefficient range. The addition of a ventral fin to the model having 20° wing dihedral and a 30° V-tail (fig. 11) resulted in a configuration having directional stability throughout the entire lift-coefficient range. The addition of the ventral alone produced a stable increment to the directional stability that was generally about the same throughout the entire lift-coefficient range as shown by the tail-off and ventral-alone data. The stabilizing contribution of the ventral was larger when used with the 30° V-tail configuration. The configuration with the V-tail at negative dihedral angles (-45, -90°, fig. 10) showed large losses in directional stability at the high-lift coefficients.

The effective dihedral increased slightly with increase in lift coefficient for the 30° V-tail configuration with a decrease in effective dihedral at the higher lift-coefficient range. The addition of the

ventral resulted in a further reduction in effective dihedral in the high-lift-coefficient range.

The data of figure 12 show the effect of various tail configurations on the lateral stability parameters for the model with wing dihedral of 50°. The directional stability parameter C_{n_β} for the model with -45° V-tail shows a small variation with increase in lift with a slight decrease in directional stability at the higher lift coefficients. The data also show that for this same configuration the variation of effective dihedral with lift coefficient was generally constant except at the higher lift coefficients where a loss occurred in effective dihedral.

CONCLUSIONS

An investigation was made in the Langley 300 MPH 7- by 10-foot tunnel to determine the low-speed static stability characteristics of a cambered-delta-wing model at dihedral angles of 0°, 20°, 33°, and 50°. The results indicate the following:

1. The tail-off longitudinal stability for the various wing dihedral angles investigated was very similar to that of the plain delta wing at zero dihedral angle.

2. Increasing the wing dihedral angle for the tail-off configuration resulted in increased directional stability with increase in lift coefficient. However, increasing the wing-dihedral angle with the tail off also resulted in rapid decreases in the effective dihedral at high-lift coefficients.

3. Proper selection of V-tail configurations which were investigated with the 20° and 50° wing-dihedral-angle configurations resulted in directionally stable configurations throughout the lift-coefficient range with only slight losses in effective dihedral at the higher lift coefficients.

The resulting model configurations also had longitudinal stability throughout the lift-coefficient range.

Langley Aeronautical Laboratory,
National Advisory Committee for Aeronautics,
Langley Field, Va., December 1, 1955.

REFERENCES

1. Sisk, Thomas R., and Muhleman, Duane O.: Lateral Stability and Control Characteristics of the Convair XF-92A Delta-Wing Airplane As Measured in Flight. NACA RM H55A17, 1955.

2. Fisher, Lewis R.: Low-Speed Static Longitudinal and Lateral Stability Characteristics of Two Low-Aspect-Ratio Wings Cambered and Twisted To Provide a Uniform Load at a Supersonic Flight Condition. NACA RM L51C20, 1951.

3. Paulson, John W.: Comparison of the Static Stability of a 68.7° Delta-Wing Model With Dihedral and a Twisted and Cambered Wing Model of the Same Plan Form. NACA RM L55B11, 1955.

4. Riebe, John M., and Fikes, Joseph E.: Preliminary Aerodynamic Investigation of the Effect of Camber on a 60° Delta Wing With Round and Beveled Leading Edges. NACA RM L9F10, 1949.

5. Brown, Clinton E., and Hargrave, L. K.: Investigation of Minimum Drag and Maximum Lift-Drag Ratios of Several Wing-Body Combinations Including a Cambered Triangular Wing at Low Reynolds Numbers and at Supersonic Speeds. NACA RM L51E11, 1951.

6. Riebe, John M., and MacLeod, Richard G.: Low-Speed Wind-Tunnel Investigation of a Thin 60° Delta Wing With Double Slotted, Single Slotted, Plain, and Split Flaps. NACA RM L52J29, 1953.

7. Riebe, John M., and Graven, Jean C., Jr.: Low-Speed Investigation of the Effects of Location of a Delta Horizontal Tail on the Longitudinal Stability and Control of a Fuselage and Thin Delta Wing With Double Slotted Flaps Including the Effects of a Ground Board. NACA RM L53H19a, 1953.

8. Gillis, Clarence L., Polhamus, Edward C., and Gray, Joseph L., Jr.: Charts for Determining Jet-Boundary Corrections for Complete Models in 7- by 10-Foot Closed Rectangular Wind Tunnels. NACA WR L-123, 1945. (Formerly NACA ARR L5G31.)

9. Herriot, John G.: Blockage Corrections for Three-Dimensional-Flow Closed-Throat Wind Tunnels, With Consideration of the Effect of Compressibility. NACA Rep. 995, 1950. (Supersedes NACA RM A7B28.)

10. Goodman, Alex, and Thomas, David F., Jr.: Effects of Wing Position and Fuselage Size on the Low-Speed Static and Rolling Stability Characteristics of a Delta-Wing Model. NACA TN 3063, 1954.

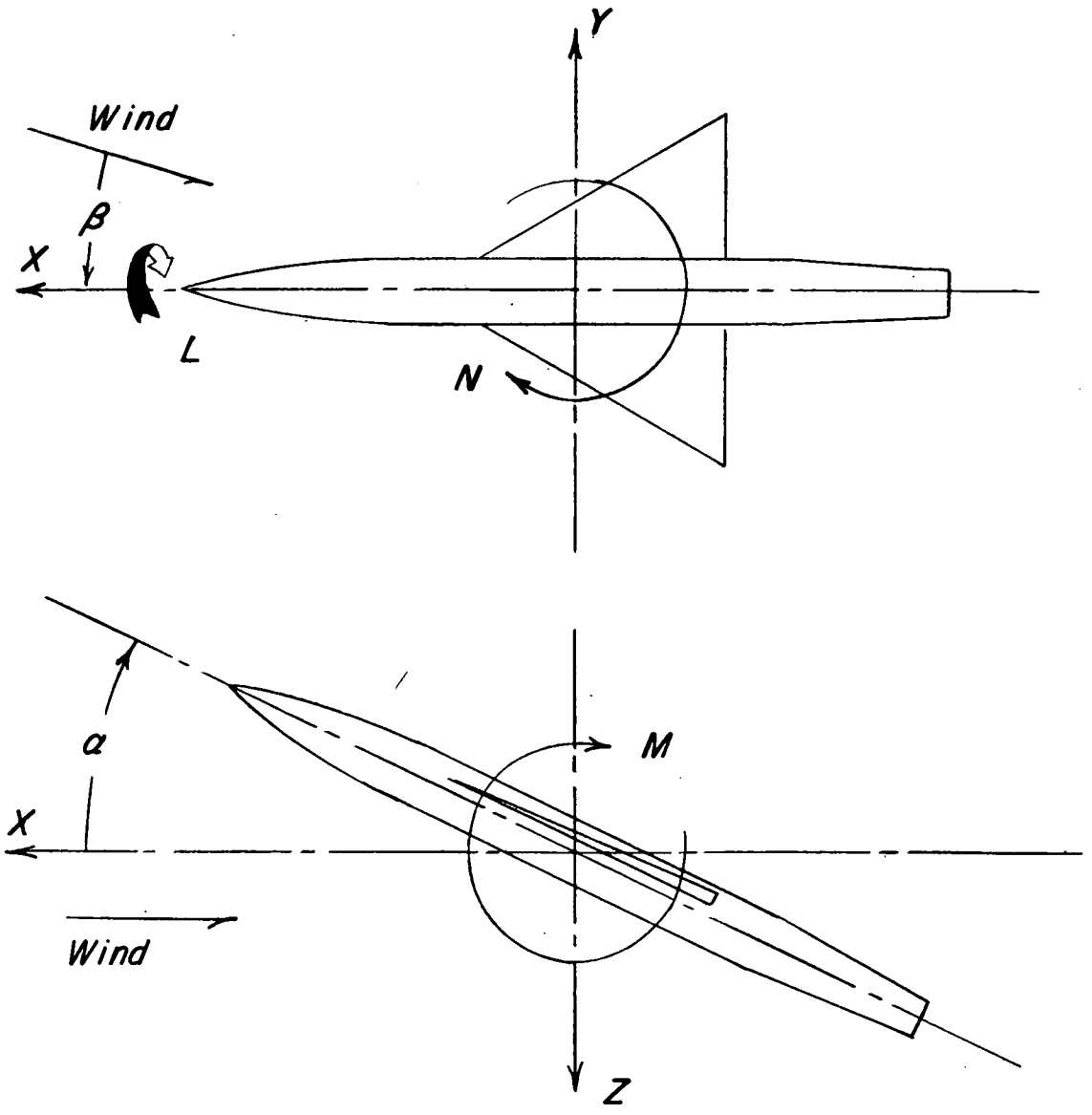

Figure 1.- System of stability axes. (Positive directions of forces and moments are indicated by arrows.)

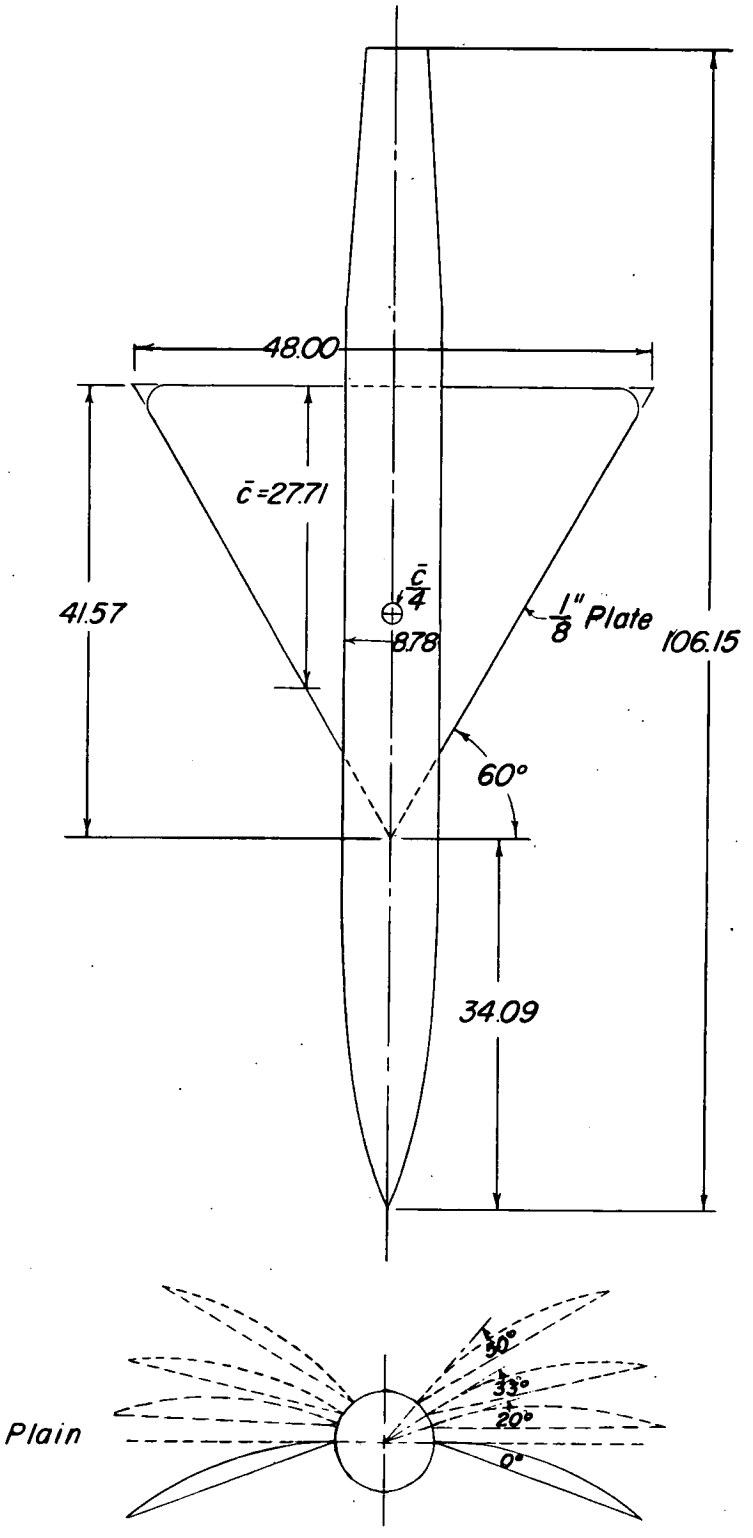

Figure 2.- Wing configurations tested on model.

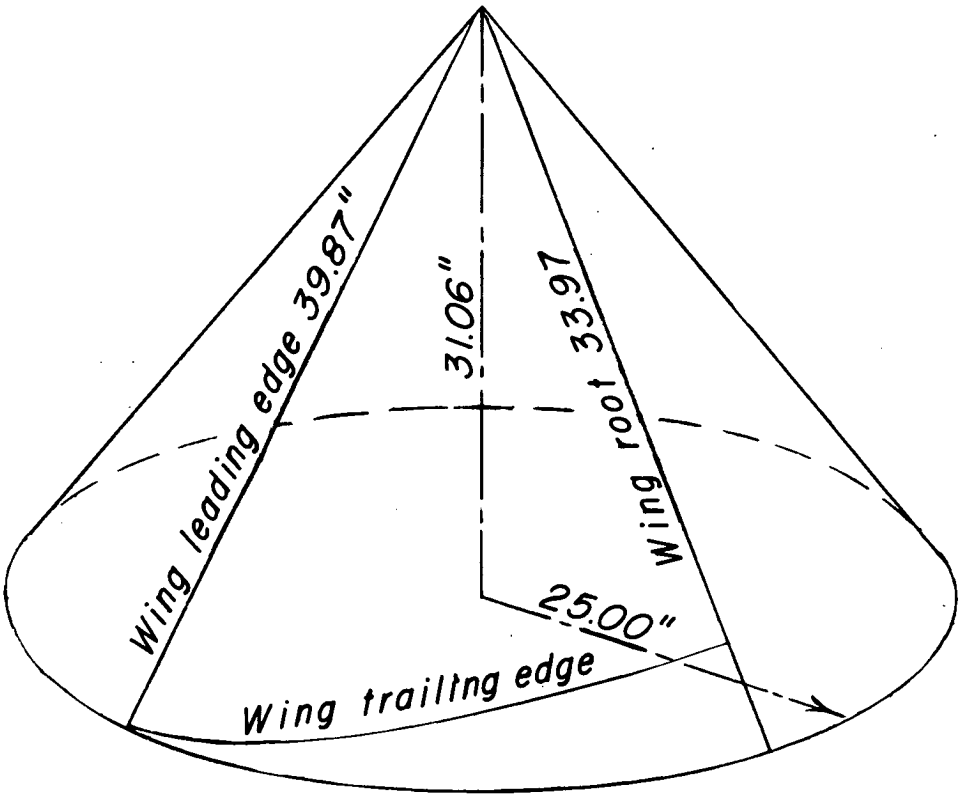

Figure 3.- Development of conical wing from right circular cone.

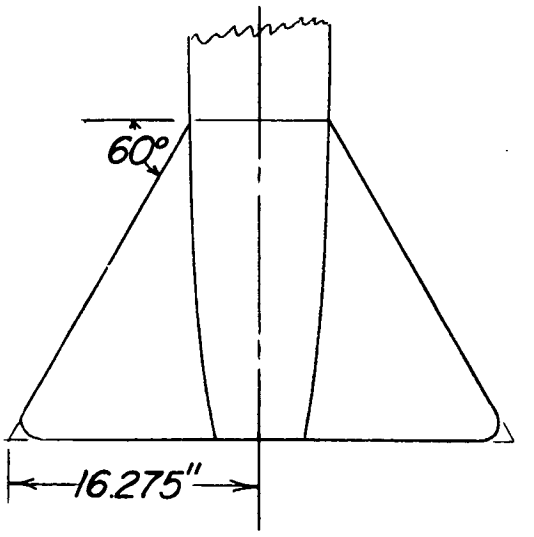

(a) Plan view of tail (0° dihedral angle).

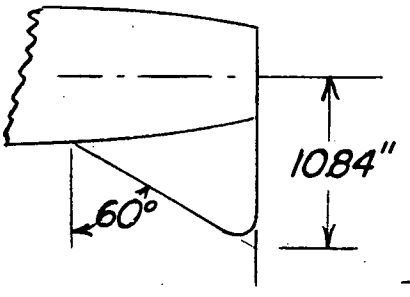

(b) Ventral fin
(tested with 30° V-tail).

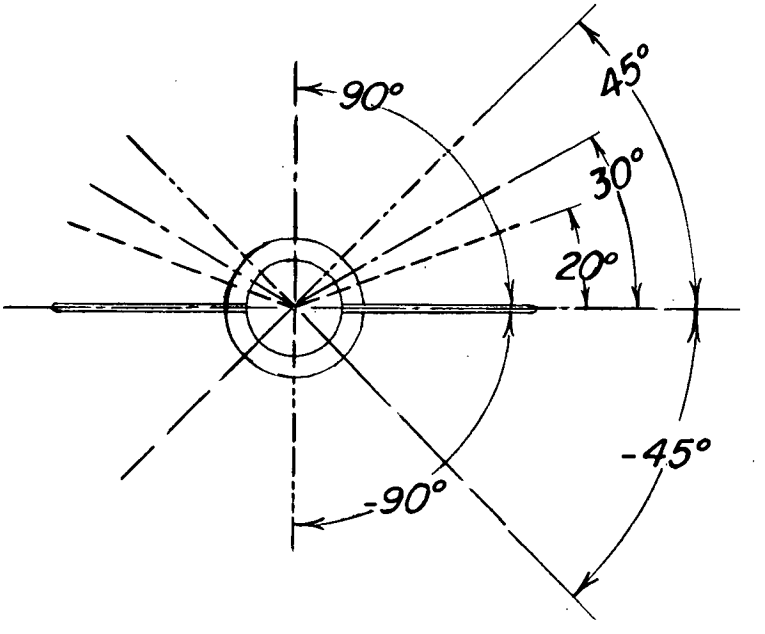

(c) Tail dihedral angles investigated.

Figure 4.- Tail configurations tested on model.

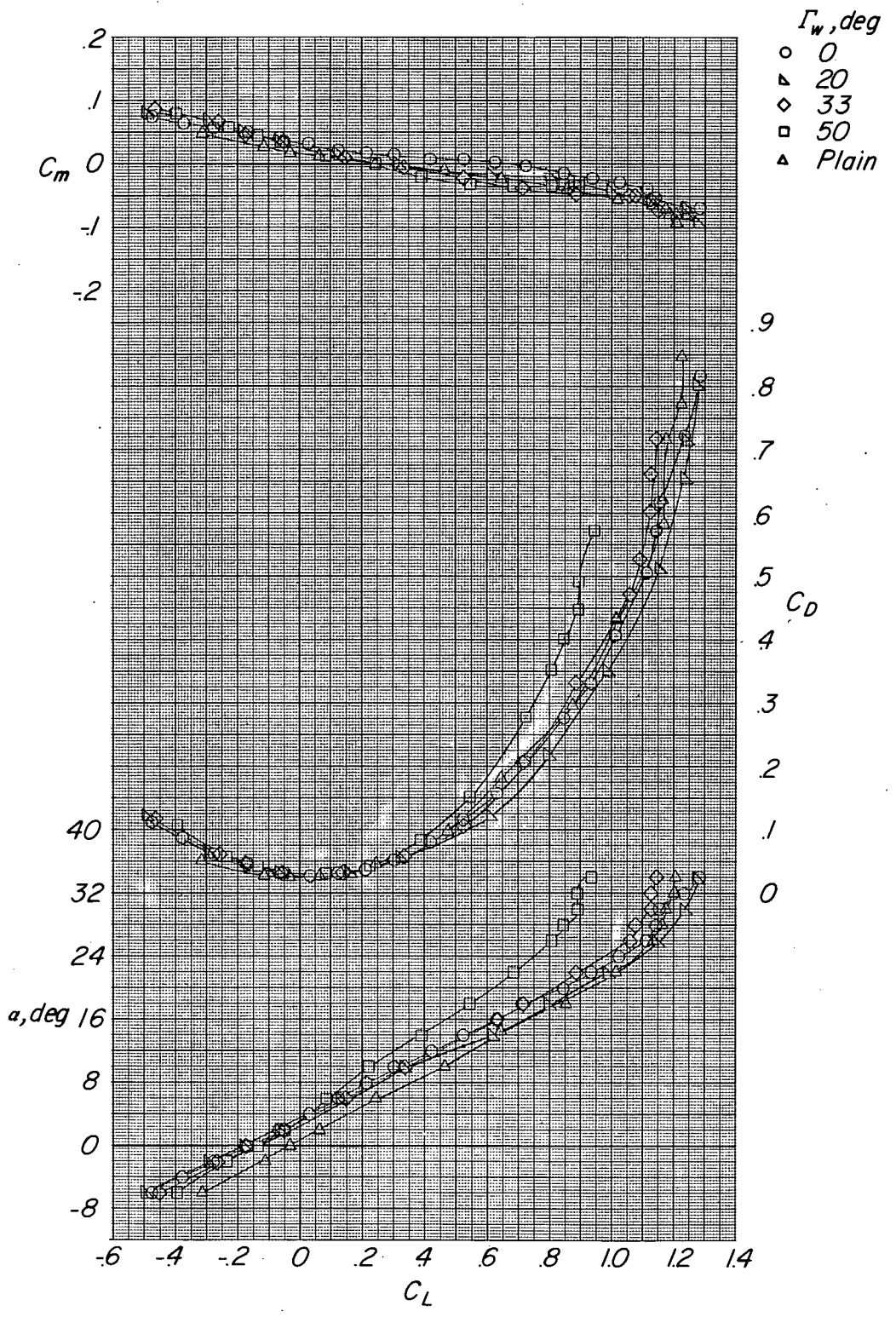

Figure 5.- Aerodynamic characteristics in pitch for various wing dihedral angles and plain delta wing; tail off.

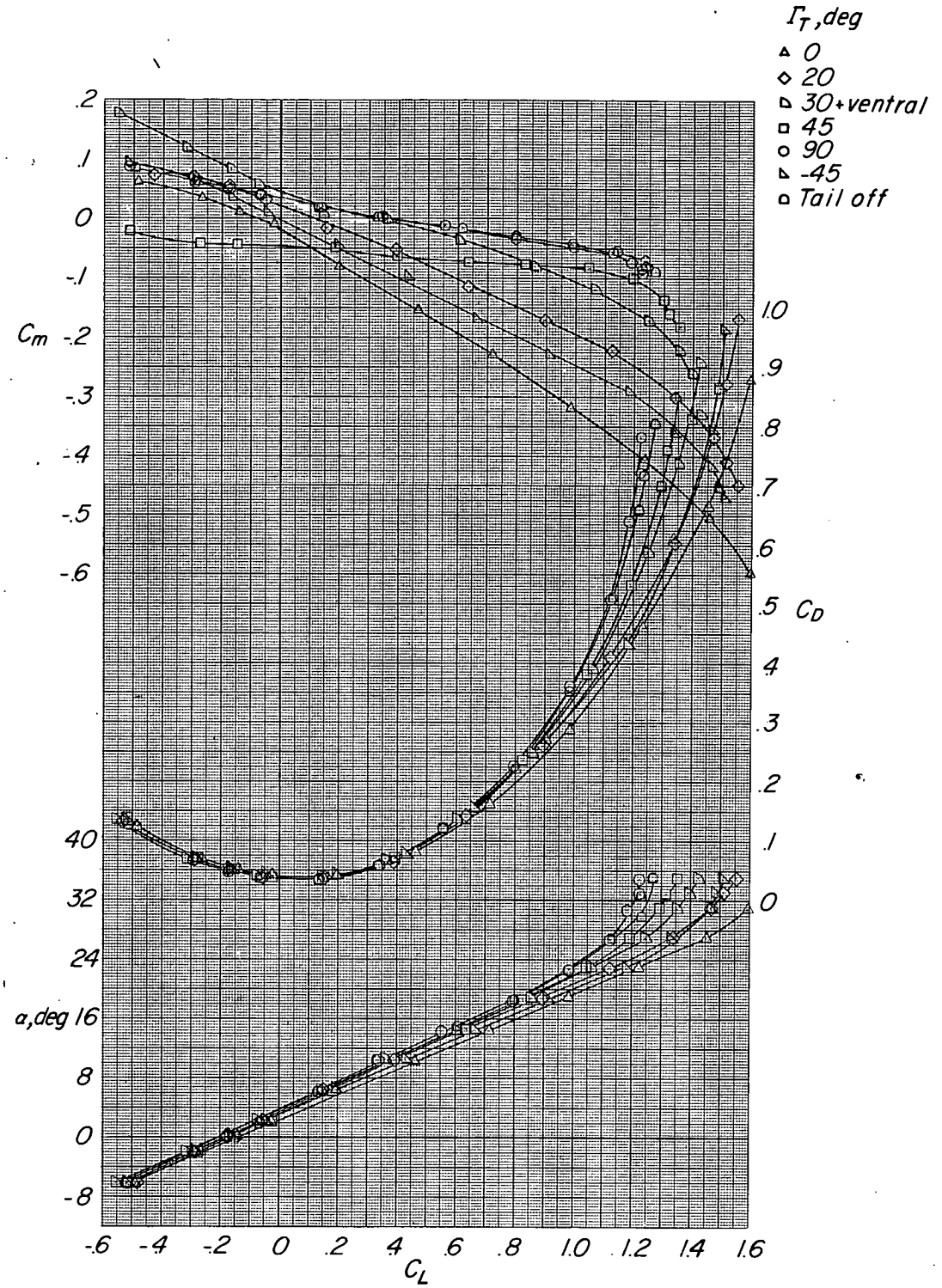

(a) $\Gamma_W = 20^\circ$.

Figure 6.- Aerodynamic characteristics in pitch for various tail configurations; $i_t = 0^\circ$.

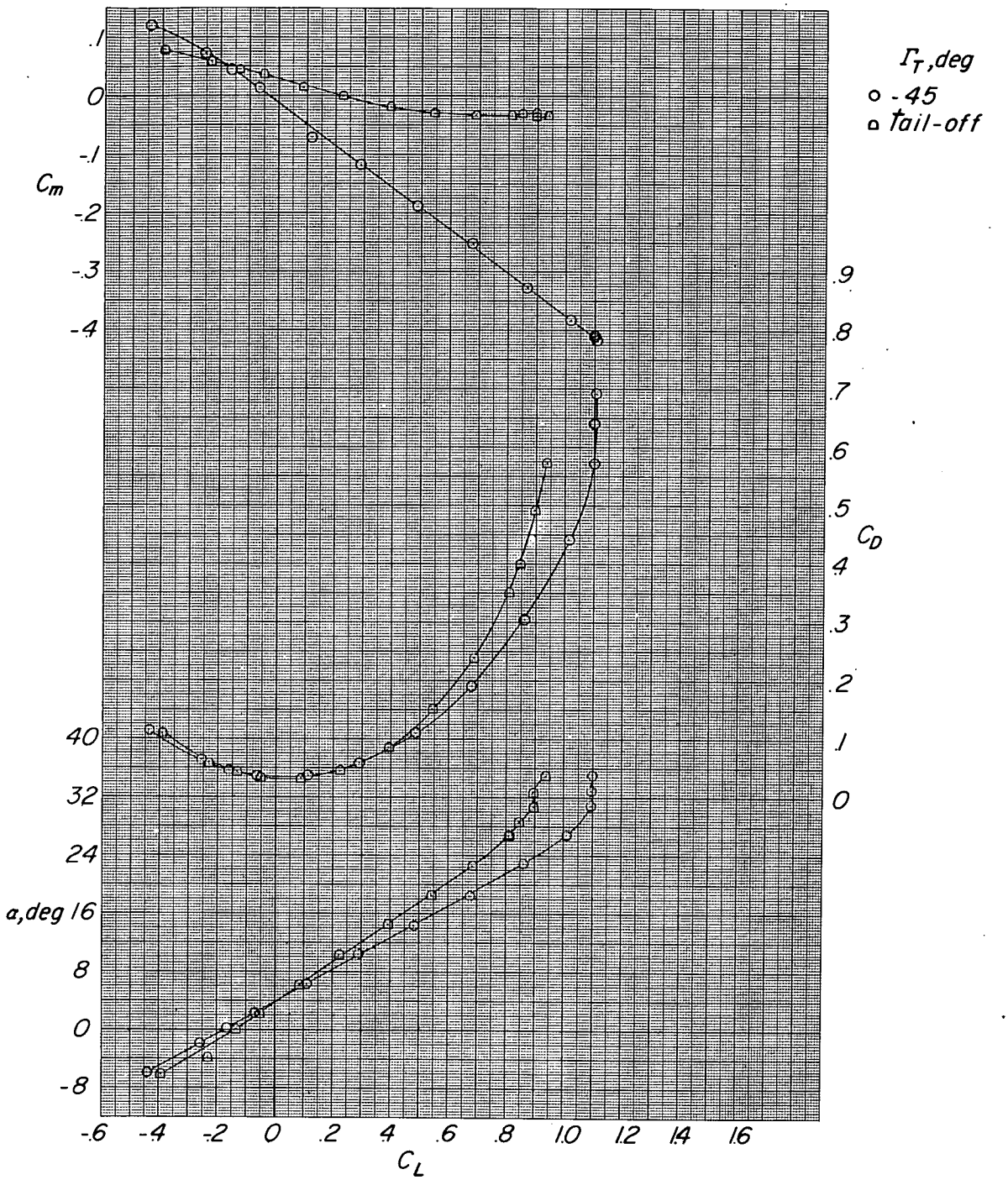

(b) $\Gamma_W = 50°$.

Figure 6.- Concluded.

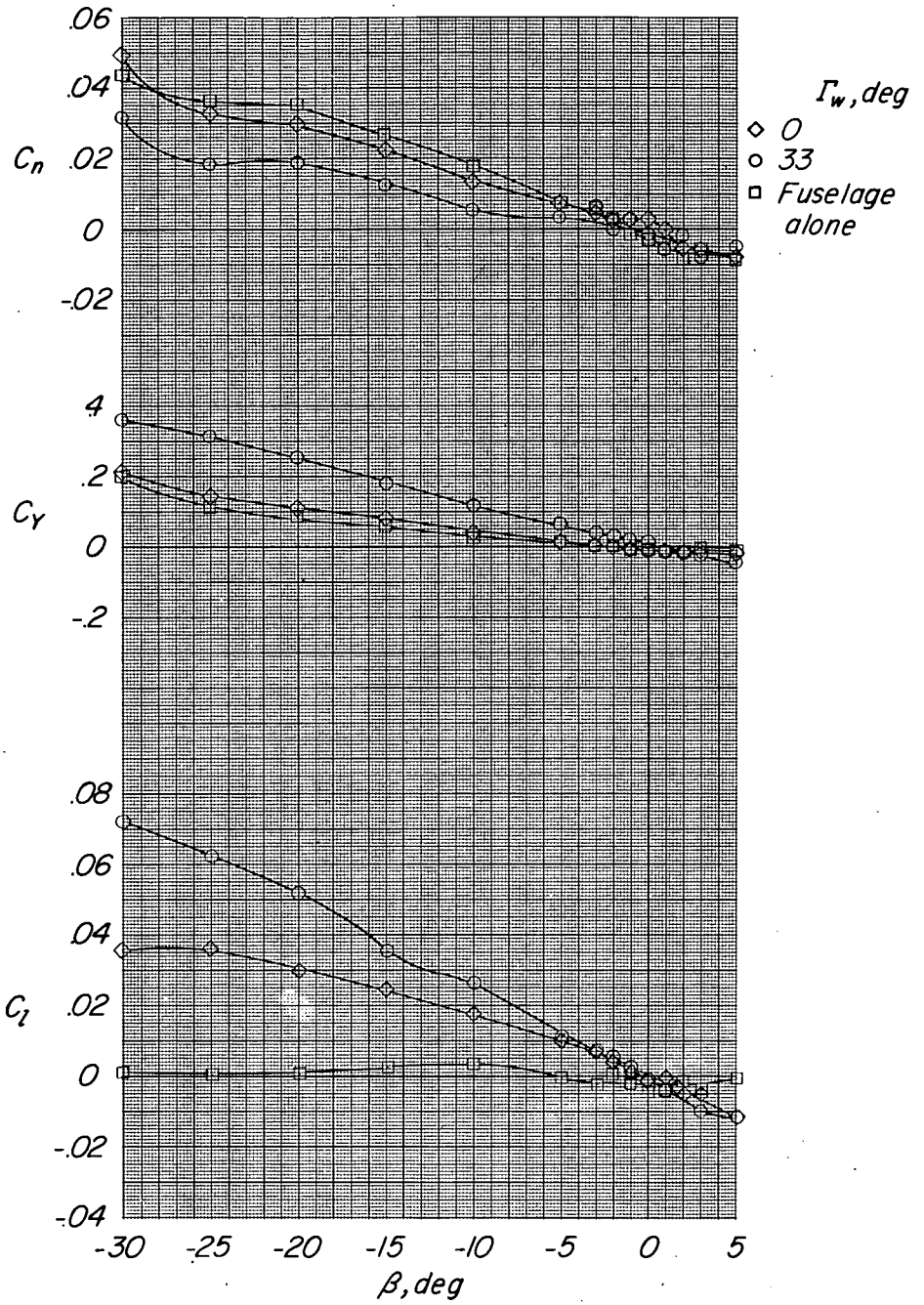

(a) Tail off.

Figure 7.- Aerodynamic characteristics with sideslip angle for 0° and 33° wing dihedral and fuselage alone; $\alpha = 10°$.

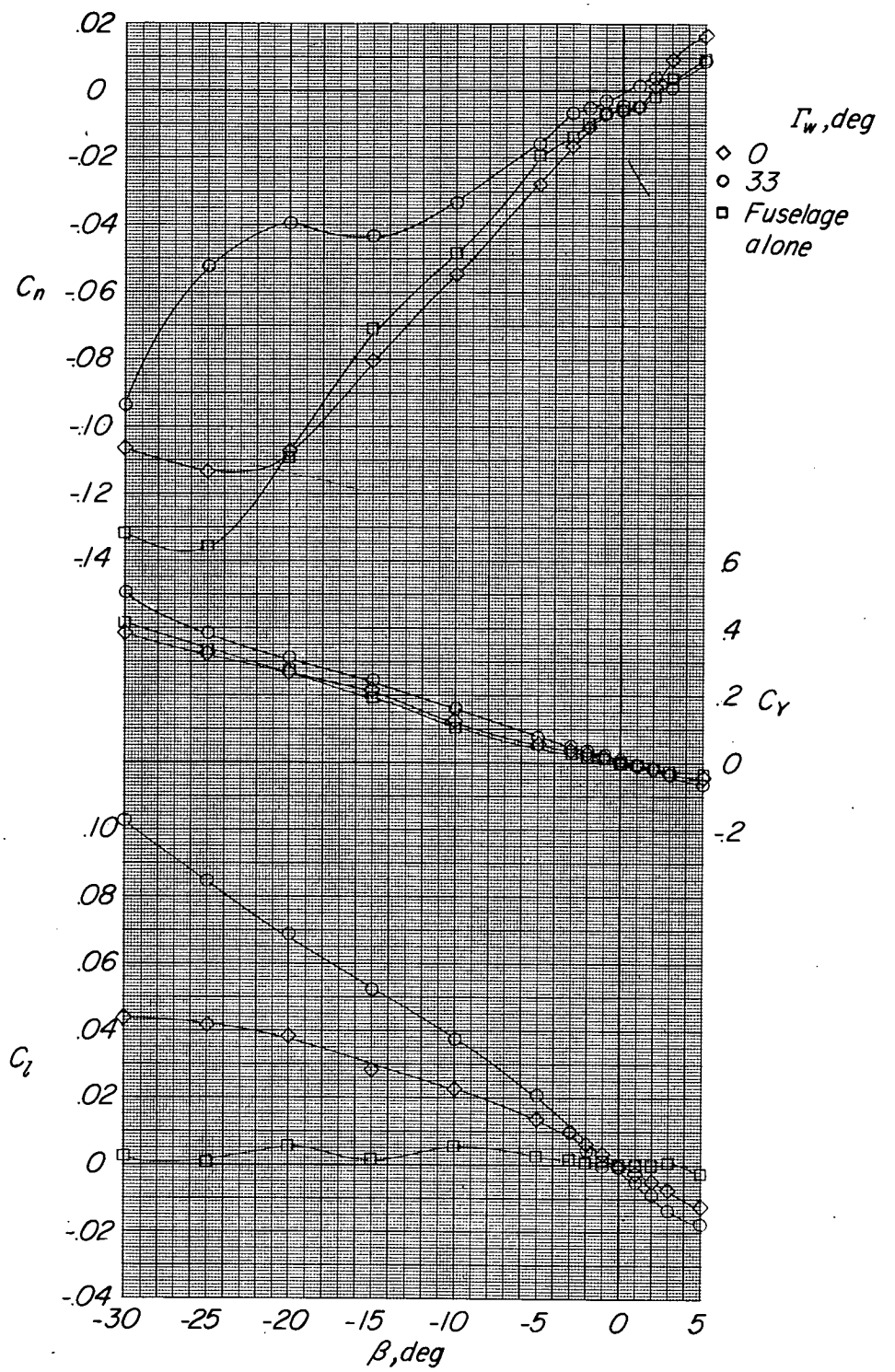

(b) With 90° V-tail.

Figure 7.- Concluded.

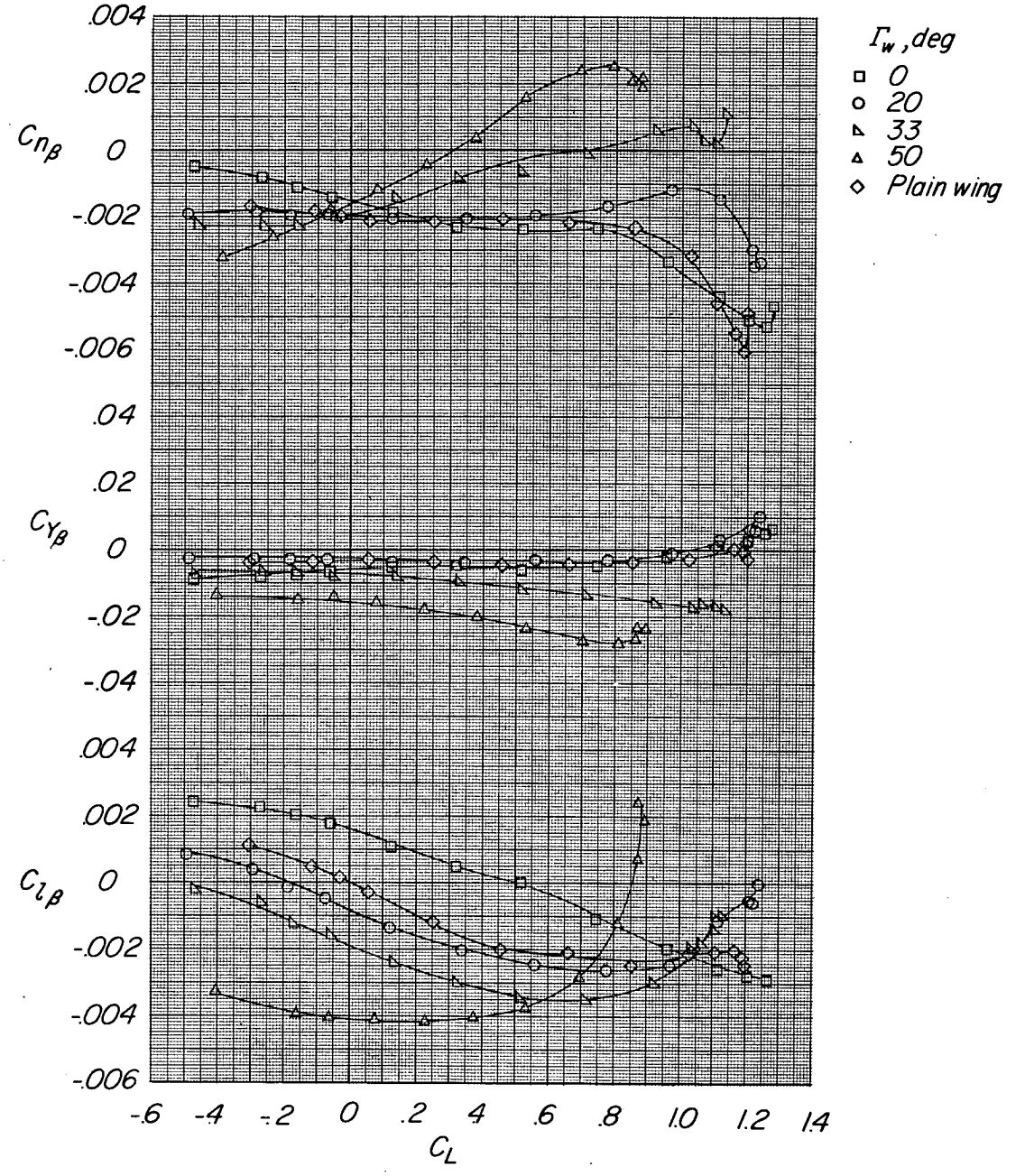

(a) Tail off.

Figure 8.- Lateral stability parameters for various wing dihedral angles.

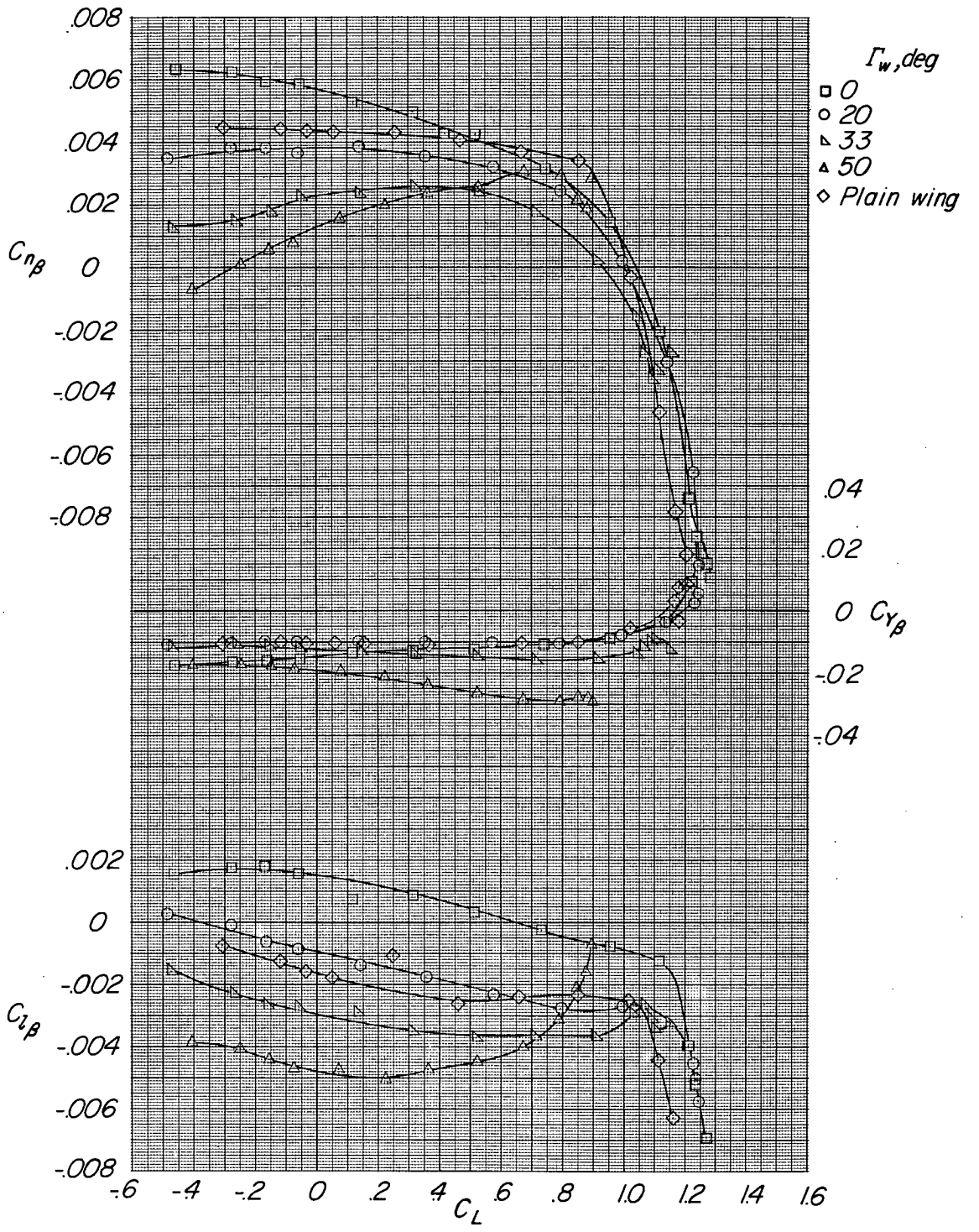

(b) With 90° V-tail.

Figure 8.- Concluded.

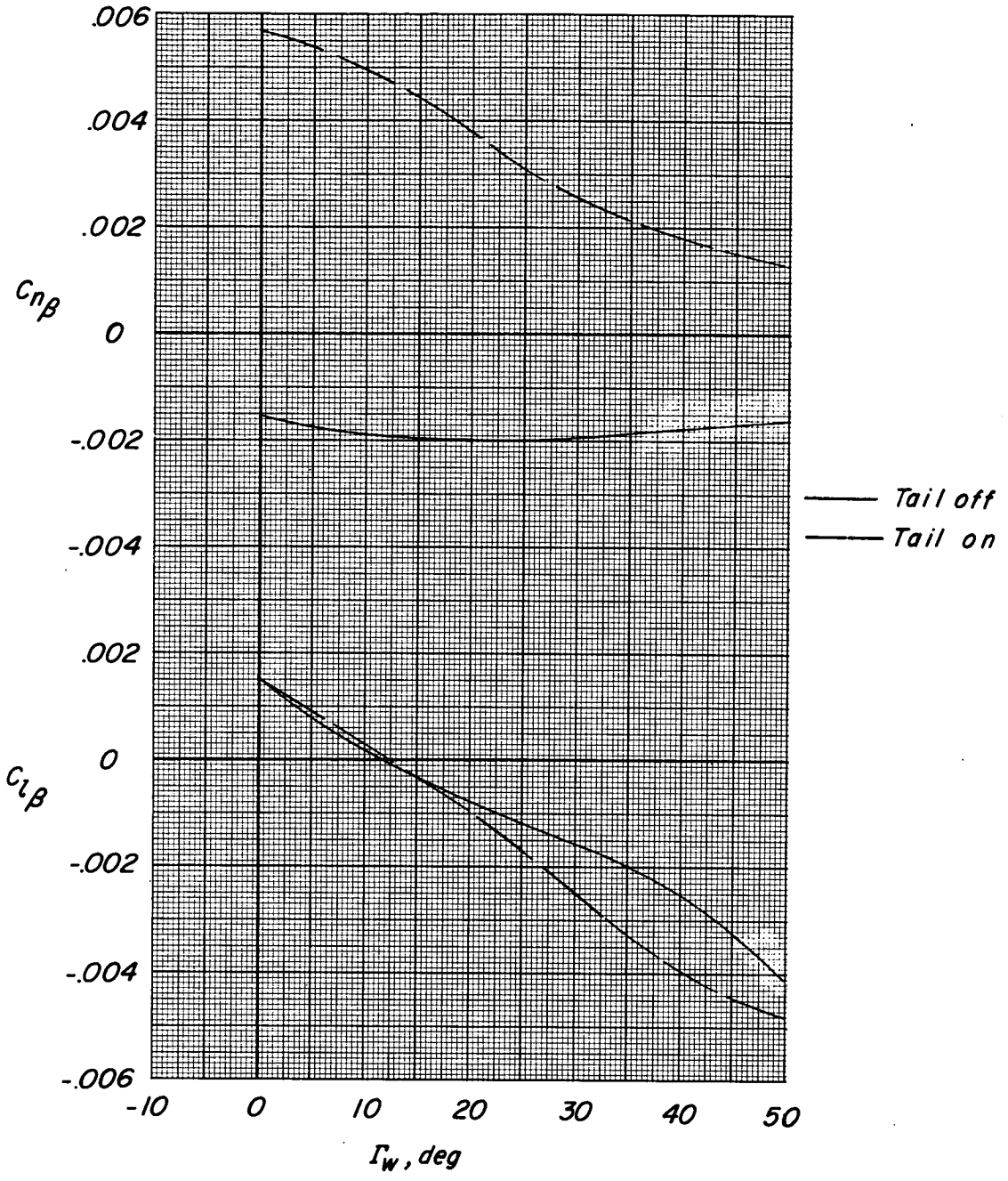

Figure 9.- Summary of lateral stability parameters with wing dihedral angle; $C_L = 0$.

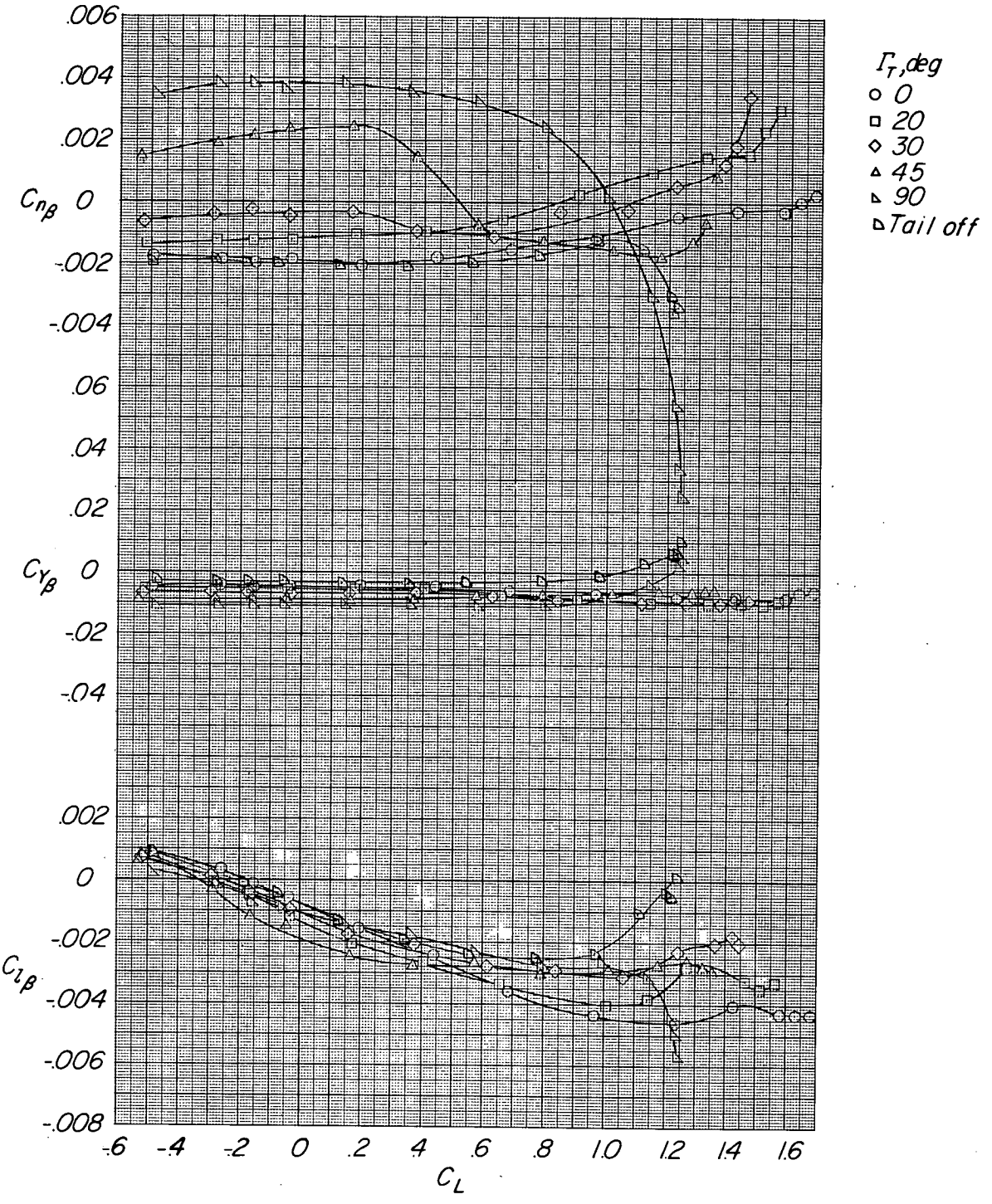

(a) Positive tail dihedral angle.

Figure 10.- Effect of dihedral angle of V-tail on lateral stability parameters; with 20° wing dihedral.

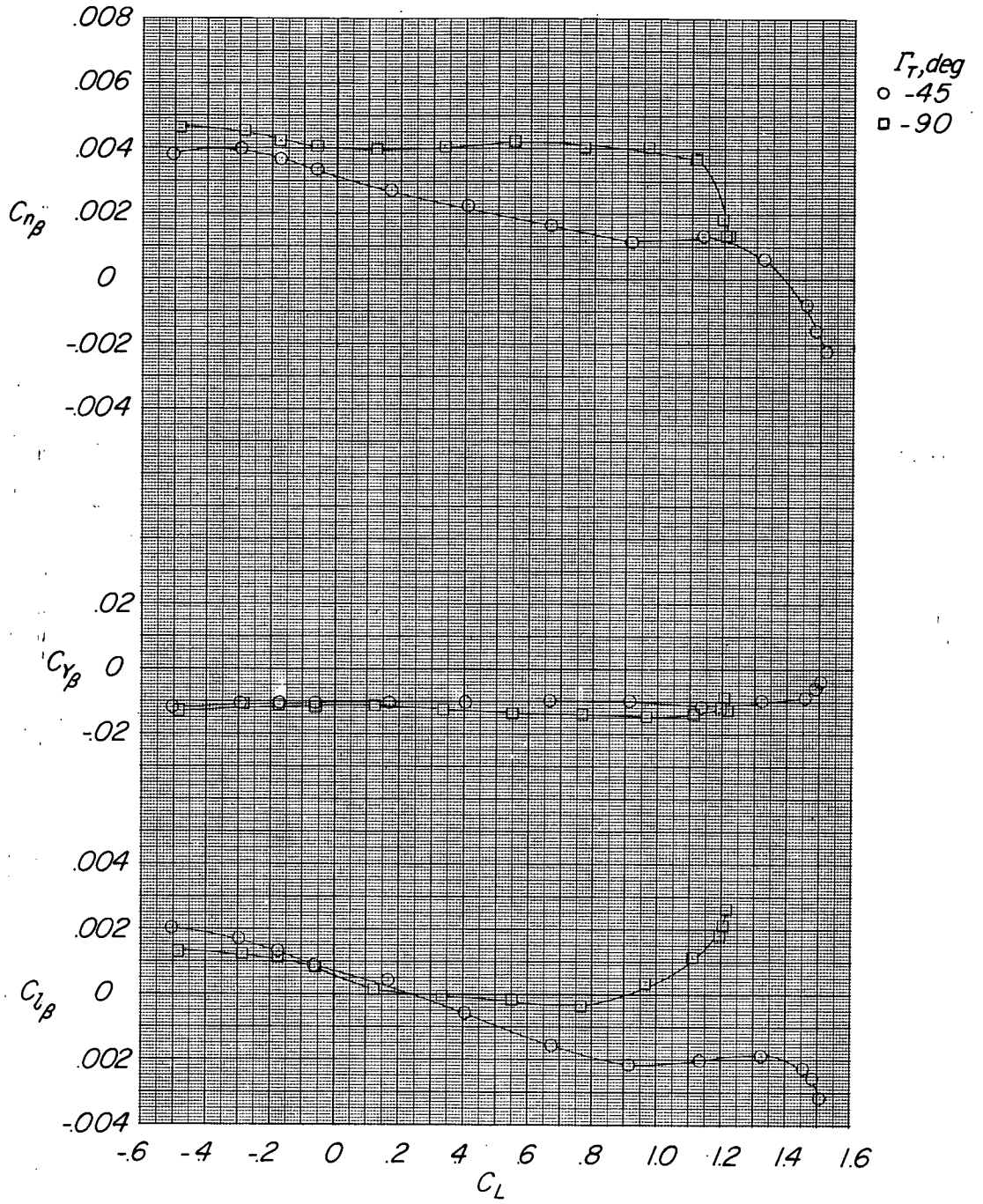

(b) Negative tail dihedral angle.

Figure 10.- Concluded.

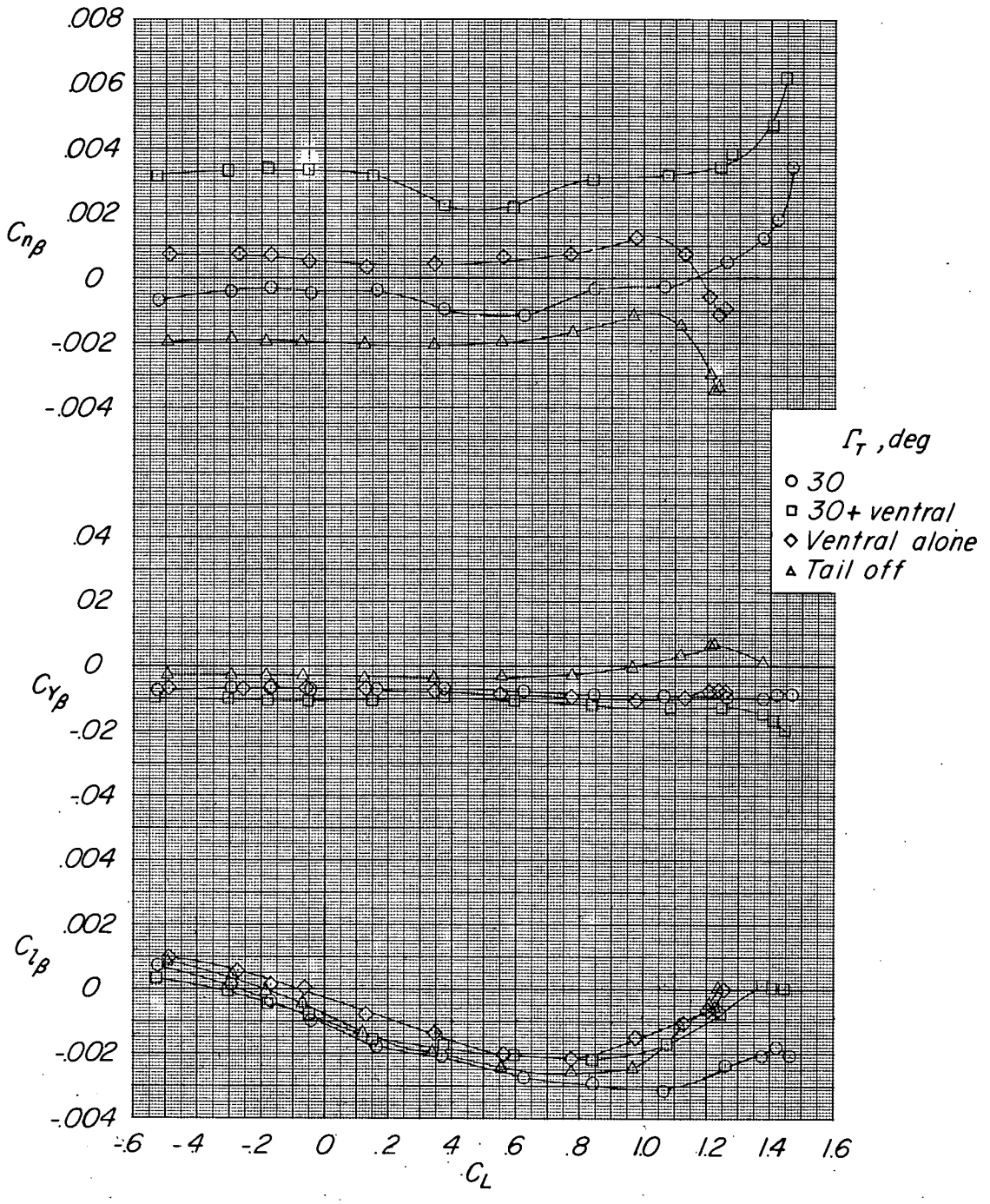

Figure 11.- Effect of ventral fin on model with 20° wing dihedral and 30° V-tail on lateral stability parameters.

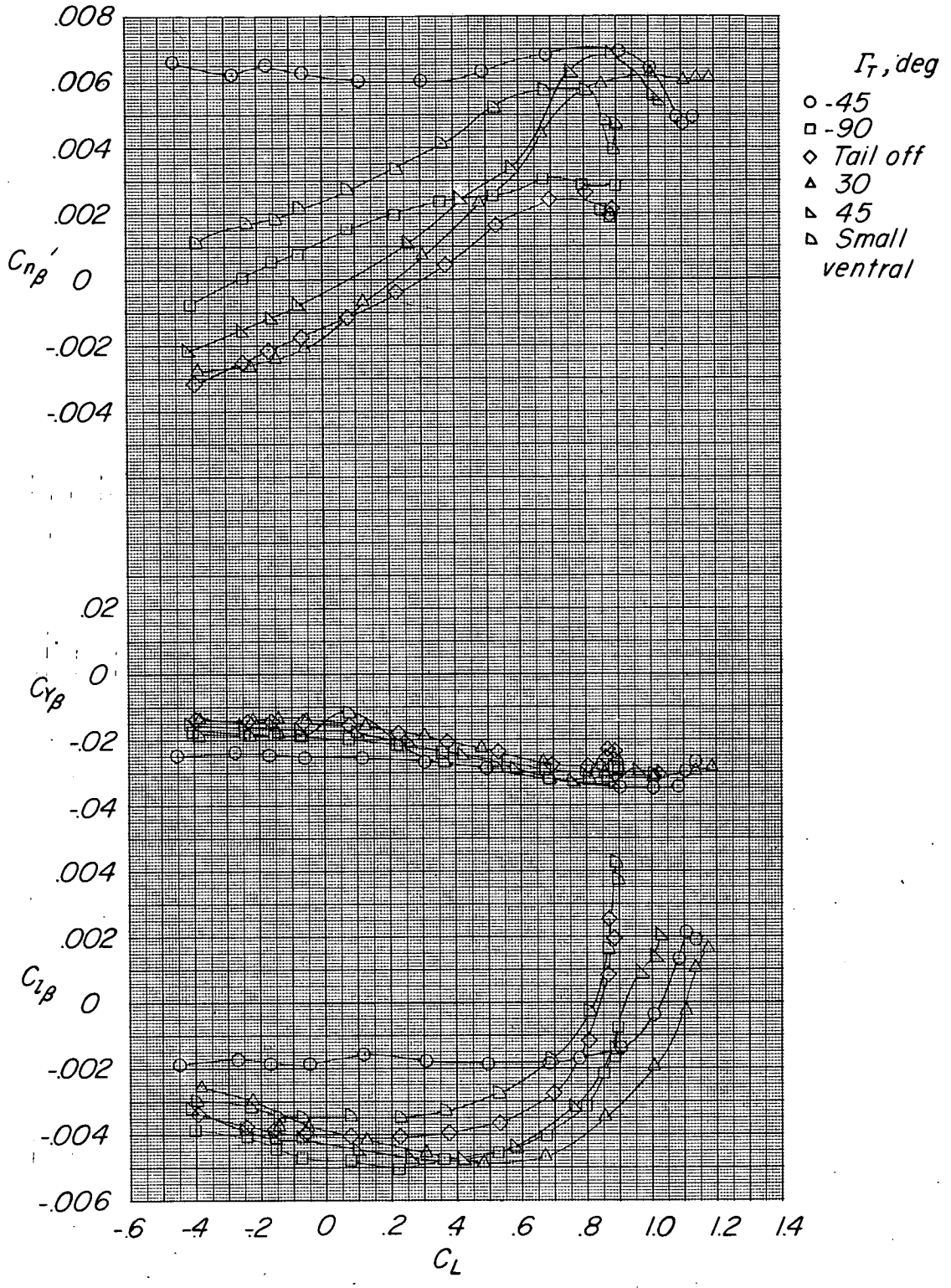

Figure 12.- Effect of various tail configurations on model with 50° wing dihedral.